by J.T.P. Castro, R.D. Vieira, R.A. Sousa, M.A. Meggiolaro, and J.L.F. Freire

DEAD LOAD EVALUATION IN REINFORCED CONCRETE COLUMNS USING RELEASED STRAIN MEASUREMENTS

A large and busy subway station was undergoing important structural modifications to be the main commuting point between an existing line and a new one under construction. Its reinforced concrete structure was built several years ago assuming the new line would have parallel tunnels to hold its two railways, but it had to be adapted as the new line was being dug by a bigger machine to settle its two railways inside a single tunnel. Consequently, several of its columns should be removed and properly replaced to allow the passage of the digging machine and the new line adjacent railways without interrupting the station services. To assure the safety of this unusual task, load measurements were required in the columns affected by the station upgrade, but as the station structure should continuously support the existing line traffic during the new line construction, alleviated strain measurements induced by localized stress releases were proposed for indirectly measuring the required loads. However, the loads calculated from the released strains in a standard linear elastic way appeared to be larger than the column's ultimate design load, causing concern about their removal process. But such approximated calculations do not include the very significant concrete creep influence on the measured strains, which is only implicitly considered by the "allowable stresses" specified in design codes. As this procedure is inappropriate for experimental stress analysis purposes, a relatively simple viscoelastic model is proposed to describe the concrete long-term stress–strain behavior. This model is extended to describe the reinforced column's behavior, and then qualified by fitting it to concrete creep data from the literature, proving that, despite their high value, the measured strains were indeed compatible with the columns' expected loads.

MEASUREMENT DETAILS

The various concrete columns were approximately 1.2 m in diameter. They were reinforced by 30 or more vertical steel rods, distributed more or less uniformly along the column perimeter. But there was no warranty about the depth of the rods, nor about the thickness of the concrete layer which covered them. Thus, to avoid the uncertainty associated with released strain measurements made on concrete layers of varying thickness (which, as it was later on verified, indeed varied significantly from column to column, and even around a same column), small holes were opened on the surface of a column's section to expose a small portion of some of their steel reinforcing bars. These had a minimum yield strain $\varepsilon_{Y\,min} > 2500\ \mu m/m$ and diameters 16, 20, or 24 mm. These bars were properly strain gaged and then sectioned to release their strains. It is worth mentioning that the rod sectioning method could be substituted by the tick-tack-toe method proposed elsewhere,[1] if the concrete layers were thick enough or if the columns were made of nonreinforced concrete.

The minimum number of distinct measuring points required to separate the strains caused by the axial load from those induced by the bending moments in any given cross section of an isotropic cylindrical column is three. But, whenever possible, gages were bonded in four of the reinforced bars more or less 90° apart to provide some measurement redundancy. This conservative practice is strongly recommended, not only to avoid losing important information in case of an eventual gage problem but also to provide some insight on the measurement dispersion. Thus, four small holes or windows were opened on the surface of most of the 28 columns examined, spaced at approximately 90° in a same transversal plane, to expose a short portion of some of their steel reinforcing bars. In a few columns, only three windows could be opened, due to access limitations, losing in this way the measurement redundancy, but still allowing the separation of the normal from the bending loads. The windows were typically around 200 mm high, and their depth and horizontal size were kept as small as possible (around 150 mm wide and 50–100 mm deep in most cases, see Fig. 1) to allow the preparation of the rod's surface for bonding the strain gage, and the subsequent cut of the lower part of the exposed rod by a 125-mm abrasive wheel.

A carefully grounded small plane recess about 8–12 mm wide and 40–60 mm long was opened in the surface of each exposed rod inside the windows, as depicted in Fig. 2. The grounded surface was finished by hand using a 220-grid sand paper. A uniaxial strain gage was then bonded on this surface using a cyanoacrilate adhesive after proper cleaning, connected to a three-wire shielded cable, and protected by a neutral silicone rubber barrier. After connecting and balancing the four (or three) gages of a column in a precision four-channel portable strain indicator, the lower part of the rods were slowly cut by the abrasive wheel, always in several steps to allow adequate water cooling during the progressive cutting, in order to avoid overheating the gage (which was easily verified by holding the rods with a bare hand). The cuts were always performed at least 100 mm (or more than 4–5 rod diameters) from the gage, and the strain readings were only made after the complete stabilization of their (small) thermal transients. Before starting any analysis, it is important to point out that the released strain measured in any steel rod can in general be due to the superposition of several mechanisms, namely:

1. The rod service stress caused by the column load, the reason for this measurement.
2. Concrete creep under the service load (the steel rods do not creep significantly at room temperature, but their strains also increase to maintain their geometrical compatibility with the slowly creeping concrete).

J.T.P. Castro (jtcastro@puc-rio.br), R.D. Vieira, M.A. Meggiolaro, and J.L.F. Freire (SEM member) are professors associated with the Mechanical Engineering Department and R.A. Sousa is a graduate student of the Civil Engineering Department, Pontifical Catholic University of Rio de Janeiro, PUC-Rio, R. Marquês de S. Vicente 225, Rio de Janeiro, RJ, 22451-900, Brazil.

doi: 10.1111/j.1747-1567.2009.00605.x

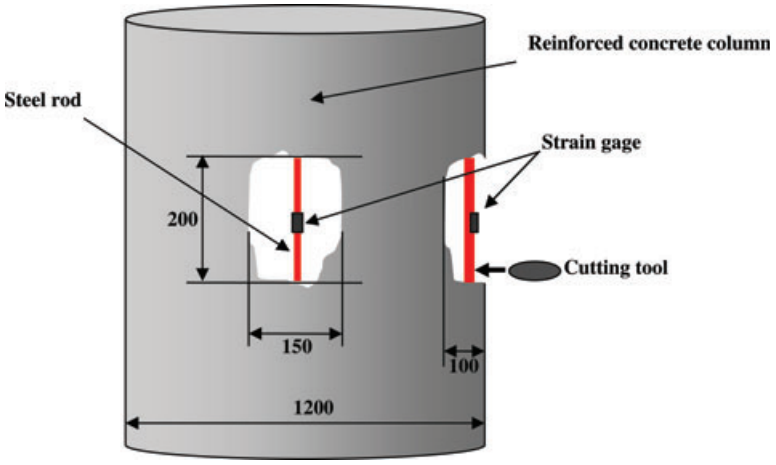

Fig. 1: Sketch of the measurement procedure (dimensions in mm)

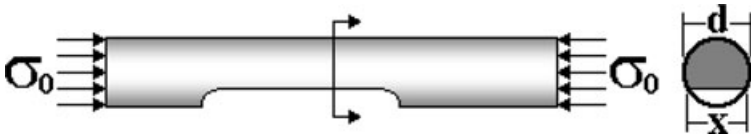

Fig. 2: The small recess for bonding the gages introduces some bending strains in the rod

3. Concrete shrinkage during its cure (with consequences similar to creep).
4. Residual stresses introduced by the rods' manufacturing process (e.g. by nonuniform plastic deformations and/or by heat treatments).
5. Residual stresses introduced during the mounting of the reinforcement.
6. Concrete removal to expose the rod for the measuring process (the load carried by that small concrete volume is partially transferred to the exposed rod) and
7. Rod cross section decrease during the preparation of its surface for bonding the gage.

The severance of a rod interrupts its force path and completely releases all these strain components under the gage, no matter which mechanisms caused them, and the rod strain alleviation can be correlated with the stress, thus with the forces that were imposed on it, if: (1) it can be supposed that the stress caused by the load in the rod is uniaxial, a reasonable assumption in such a slender member built into a concrete column of a much larger diameter; and (2) if all the other strain parcels can be neglected or properly evaluated. As the sectioning cuts were made several rod diameters from the gages, the self-equilibrating residual stresses introduced during the rod's manufacture should not significantly affect the gage measurements according to Saint Venant's principle, thus component 4 of the above list could be safely neglected. As all four (or three) gages of a given column were continuously monitored during the cutting process, it could be observed that cutting a rod did not influence the others, which remained balanced within the strain indicator noise level (less than $\pm 5\,\mu$m/m). Therefore, the column stiffness loss introduced by alleviating the instrumented rods was negligible, and so was the sixth listed component of the total rod strain. All the exposed rods were checked for lateral displacements and/or rotations after the cuts, but they maintained the alignment in almost all cases, evidence that the mounting stresses which could cause the fifth listed strain component were also negligible. Finally, the effect of the rod cross-section reduction shown in Fig. 2 could easily be accounted for.

The grinding of a small plane recess is required to bond the gages because reinforcing rods have rough surfaces with a helical thread to improve their adherence to the concrete, but they reduce the rod cross section and introduce eccentricity on their (assumed) pure compression load, thus local bending. The exposed rods are actually loaded by the strain imposed by the column, but the recess is small and can be modeled as if it was working under a pure axial load. Thus, if σ_0 is the nominal compression stress in the original reinforcing rod section of diameter d and area $A_0 = \pi d^2/4$, and if $A = d^2(\alpha - \sin\alpha \cdot \cos\alpha)/4$ is the area of the recess section of width x; $I = (d^4/64)[\alpha - \sin\alpha\cos\alpha + 2\sin^3\alpha\cos\alpha - (16\sin^6\alpha)/9(\alpha - \sin\alpha\cos\alpha)]$ is the recessed section inertia moment about a central axis parallel to the recess plane, where $\alpha = \pi - \arcsin(x/d)$ is the central angle of the recess; $y_1 = (d/2)[(2\sin^3\alpha)/3(\alpha - \sin\alpha\cos\alpha) -$

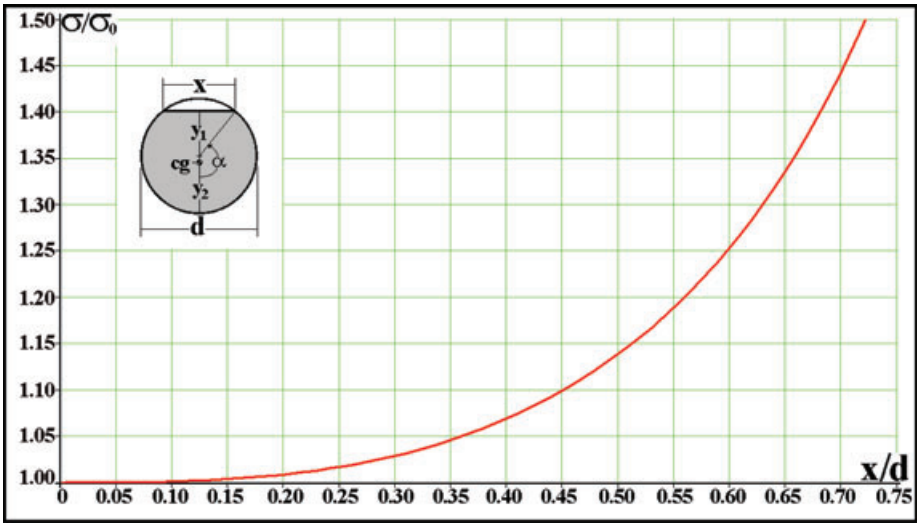

Fig. 3: Ratio σ/σ_0 as a function of the recess width x for the three rod diameters: this effect is not negligible in most cases, and it must be accounted for in the load analysis

$\sin\alpha\cos\alpha]$ and $y_2 = (d/2)[1 - (2\sin^3\alpha)/3(\alpha - \sin\alpha\cos\alpha)]$ are the distances of the recessed section centroid to the recess plane and to the opposite frontier point,[2] then the stress ratio σ/σ_0 under the gage (due to the normal and to the bending component), which is plotted in Fig. 3, is given by:

$$\frac{\sigma}{\sigma_0} = \left[\frac{A_0}{A} + \frac{A_0(d/2 - y_2)y_1}{I}\right] \tag{1}$$

The mean value of the released strains measured after sectioning more than 100 rods of 28 reinforced concrete columns was $\varepsilon_m = 1325\ \mu m/m$, and the maximum was $\varepsilon_{max} = 2600\ \mu m/m$. These strains are still within the linear elastic range of the steel rods (except for ε_{max} that is slightly above $\varepsilon_{Y\,min}$), but they seem to be too large for the concrete, whose ultimate design compressive strain is usually taken as $\varepsilon_{Uc} = 2000\ \mu m/m$. Even after considering the recess correction, which decreased the measured strain values in average by 20%, in a first look they still would imply that the columns were or could be unsafe. But there was no other evidence of such a problem, since no cracking, spalling, or any other warning was ever emitted by the columns. Moreover, the columns supported the opening of the holes and the sectioning of the instrumented rods without any problem (as stated before, the instrumented rods did not feel the sectioning of the other rods). On the other hand, there was no evidence of any problem with the measured strains. The careful measurements followed reliable and very well-established procedures, including electrical tests of the reading equipment with high-precision resistors and operational tests of the installed gages, always generating consistent checks. Therefore, something had to be done to make sense out of these two apparently incompatible, but very strong evidences, as explained below.

THE VISCOELASTIC BEHAVIOR OF CONCRETE

Concrete can creep a lot despite being made by mixing ceramic materials (gravel, sand, and a calcium silicate cement powder) with water, which hydrates and hardens the cement to form a rock-like composite. For example, Fig. 4 shows some concrete creep data presented by Leet.[3] According to Buyukozturk,[4] concrete creep is influenced by factors that can be internal, dependent on the concrete composition (such as concentration, stiffness, grading, distribution and permeability of the aggregate, water/cement ratio, cement type, etc.), or external, dependent on structural parameters (size, shape, environment, loading, etc.). Moreover, creep strains are linearly proportional to the stress if $\sigma < f'_c/2$, where f'_c is the concrete compressive strength, usually measured after a 28-day curing time. The three curves shown in Fig. 4 show only the creep compressive strains measured under 2.1, 4.2, and 6.3 MPa, which after 600 days are $\varepsilon_{cr} = 446, 872$, and $1325\ \mu m/m$, but the total strain has also an initial elastic part $\varepsilon_{el} = \sigma/E = 100, 200$, and $300\ \mu m/m$, respectively. Thus, the creep strains are *not* negligible in these tests. Moreover, the creep strains are indeed linearly proportional to the stresses, as shown in Fig. 5, where the curves obtained under 2.1 and 4.2 MPa practically coincide with the 6.3-MPa curve when multiplied by 3 and 1.5, respectively.

The next step is to find a proper rheological model to reproduce all these curves, which should not include the elastic strains as they show only the creep strains. A first option could be to try to fit the data by a Kelvin–Voigt equation, but as the experimental creep data do not show a horizontal asymptote, at least another damper is needed in the model. Any nonlinear curve can be fitted to a set of data by minimizing its mean square deviation from that set using the Levenberg–Marquardt (LM) algorithm:[5,6]

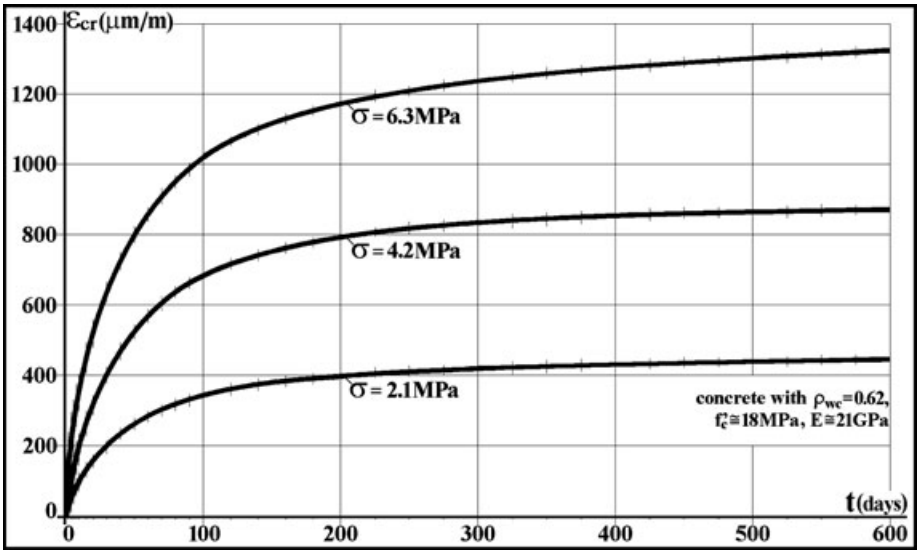

Fig. 4: Time variation of creep strains under compressive stresses for a concrete with f'_c=18 MPa,[3] Young's modulus $E_{c28} \cong 1.36\sqrt{\rho_c^3 \cdot f'_c} \cong 21$ *GPa* (both measured, as usual, 28 days after casting), water/cement ratio $\rho_{wc} = 0.62$, and density $\rho_c \cong 2.3$. The stresses and strains are plotted as positives for convenience

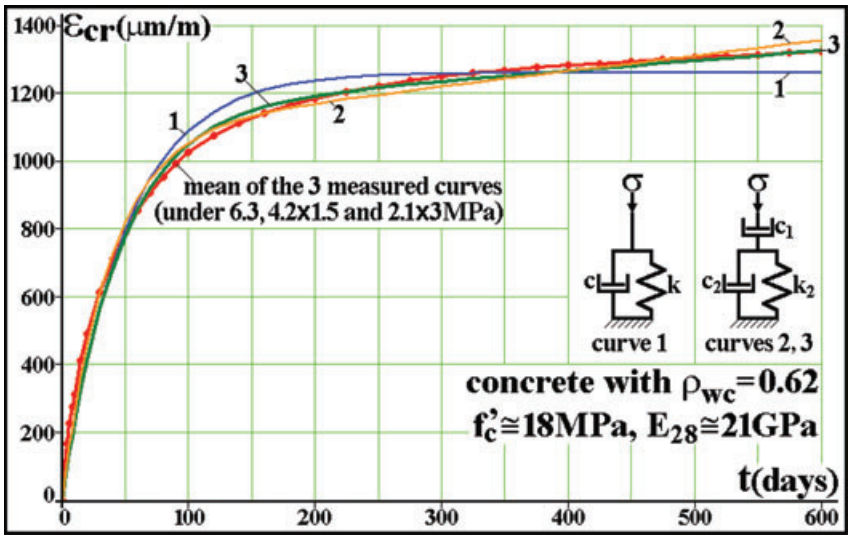

Fig. 5: Fitting of Fig. 4 concrete creep data using two linear viscoelastic models

given a set of m points (x_i, y_i), $i = 1, \ldots, m$, LM searches for the parameters' vector $p = [p_1, p_2, \ldots, p_n]^T$ (where T means transpose) containing the n constants of the specified $f(x_i, p)$ function, which minimizes the sum of the square deviations:

$$S(p) = \sum_{i=1}^{m} [y_i - f(x_i, p)]^2 \qquad (2)$$

LM can be applied to nonlinear vectorial functions, whereas x_i can be a scalar for one-variable functions, or a vector for functions of more than one variable. But in the following formulation, $f(x_i, p)$ and y_i are supposed scalars. It is didactic to present a few examples, for example, in fatigue: in Paris' rule $da/dN = f(x_i, p) = A_p \cdot \Delta K^{mp}$, $x_i = \Delta K$, and $p = [A_p, m_p]^T$; in Walker's rule $da/dN = f(x_i, p) = A_w \cdot \Delta K^{mw}/(1 - R)^{pw}$, $x_i = [\Delta K, R]^T$, and $p = [A_w, m_w, p_w]^T$; and in Coffin-Manson's rule $\Delta\varepsilon = f(x_i, p) = (2\sigma_c/E)(2N)^b +$

$(2\varepsilon_c)(2N)^c$, $x_i = N$, and $p = [\sigma_c, E, b, \varepsilon_c, c]^T$. LM is an iterative procedure, which depends on an initial estimate for the vector p, which for highly nonlinear functions needs to be close to the final solution to guarantee convergence. But this normally is not necessary for fitting data obtained in mechanical tests. In each iteration, p is replaced by a new estimate $p + q$. To find the vector $q = [q_1, q_2, \ldots, q_n]^T$, the functions $f(x_i, p + q)$ are approximated by their linearizations, given by:

$$f(x_i, p + q) \cong f(x_i, p) + J(x_i, p) \cdot q \tag{3}$$

where J is the Jacobian of f with respect to p:

$$J(x_i, p) = \left[\frac{\partial f(x_i, p)}{\partial p_1}, \frac{\partial f(x_i, p)}{\partial p_2}, \ldots, \frac{\partial f(x_i, p)}{\partial p_n} \right] \tag{4}$$

In the case discussed here, as f is scalar, the Jacobian results in the gradient of f with respect to p. When the sum of the deviations $S(p)$ is minimum, the gradient of S with respect to q is equal to zero. Therefore, applying Eq. 2 at $S(p + q)$, and making $\partial S / \partial q = 0$, results in:

$$\sum_{i=1}^{m} \{J(x_i, p)^T \cdot J(x_i, p)\} \cdot q = \sum_{i=1}^{m} \{J(x_i, p)^T \cdot [y_i - f(x_i, p)]\} \tag{5}$$

In this manner, the correction vector q can be obtained in each iteration by:

$$q = \left[\sum_{i=1}^{m} J(x_i, p)^T \cdot J(x_i, p) \right]^{-1} \cdot \sum_{i=1}^{m} \{J(x_i, p)^T \cdot [y_i - f(x_i, p)]\} \tag{6}$$

The m experimental data points can be stacked in an $m \times n$ matrix J_t and in an $m \times 1$ error vector e_t, defined as:

$$J_t(p) \equiv \begin{bmatrix} J(x_1, p) \\ J(x_2, p) \\ \vdots \\ J(x_m, p) \end{bmatrix} \quad \text{and} \quad e_t(p) \equiv \begin{bmatrix} y_1 - f(x_1, p) \\ y_2 - f(x_2, p) \\ \vdots \\ y_m - f(x_m, p) \end{bmatrix} \tag{7}$$

Then, Eq. 6 can be rewritten as:

$$q = (J_t^T J_t)^{-1} J_t^T \cdot e_t \equiv pinv(J_t) \cdot e_t \tag{8}$$

where $pinv(J_t)$ is known as the pseudo-inverse of J_t, with $pinv(J_t) \equiv (J_t^T J_t)^{-1} J_t^T$. After finding q in each iteration and summing it to the current p estimate, the algorithm continues updating p until the correction q has absolute value smaller than a given tolerance. If f varies linearly with p, then J does not depend on p, and the algorithm converges in only one iteration. Even when J depends on p, the use of a log-log scale usually guarantees convergence in a few iterations. It is advisable to monitor the value of the deviation sum $S(p)$, which should always decrease at each iteration. If $S(p)$ increases in some iteration, a possibility when working with highly nonlinear functions, it is necessary to introduce a positive damping term λ in the pseudo-inverse:

$$q = (J_t^T J_t + \lambda I)^{-1} J_t^T \cdot e_t \tag{9}$$

where I is the identity matrix $n \times n$. The damping factor λ is updated at each iteration. If the $S(p)$ reduction is too high, smaller values are chosen for λ to avoid having the algorithm become unstable. On the other hand, if $S(p)$ decreases too slowly, λ is increased to accelerate the convergence of the iterative calculations.

Marquardt[6] recommends that damping be introduced in the numerical calculation algorithm for calculating the correction vector q by guessing an initial value $\lambda = \lambda_0 > 0$ and a correction factor $v > 1$, for example, $\lambda = 1$ and $v = 2$. In this case, the vector q is calculated using a damping factor λ / v at each iteration. If $S(p + q) < S(p)$, then this q is summed to p, $\lambda = \lambda / v$ is chosen as the new factor, and a new iteration is made. In the opposite case, q is recalculated using λ. If $S(p + q) < S(p)$, then this q is summed to p, λ is maintained, and a new iteration begins. If in both cases $S(p + q) \geq S(p)$, then q is recalculated with damping factors $\lambda \cdot v^k$, k=1, 2, . . . , at each new iteration until obtaining $S(p + q) < S(p)$. When this occurs, then this q is summed to p, $\lambda = \lambda \cdot v^k$ is chosen as the new damping factor, and the iterations continue. With this procedure, the algorithm stability is guaranteed.

Two viscoelastic models are used to fit the average of the properly multiplied curves shown in Fig. 5, using the above procedures. The first model is Kelvin–Voigt's, with its two parameters k and c obtained by minimizing the mean square error, generating curve 1. The second is a Kelvin–Voigt model in series with a damper, generating curves 2 and 3, either by applying the same method or by visually refitting the parameters c_1, c_2, and k_2, respectively. The introduction of a damper in series with the Kelvin–Voigt element improves the data fitting, but the "optimum" mathematical adjustment is not as good as the old-fashioned eye-ball data fitting used to obtain curve 3. This visual tuning of the parameters generated by LM is a much recommended procedure, since there is no substitute for a well trained human judgment: the eye-ball fitting does not minimize the least square error, however, it ended up fitting better the long-term creep behavior, especially after 500 days. But such a refinement by man-machine interaction is only possible after knowing the mathematically optimized parameters. The parameters generated by the LM algorithm are $k = 5$ GPa and $c = 21.6$ GPa·s for curve 1; and $c_1 = 1.196$ TPa·s, $k_2 = 5.8$ GPa, and $c_2 = 18.92$ GPa·s for curve 2, whereas the visual refinement used to fit of curve 3 generates $c_1 = 1.814$ TPa·s, $k_2 = 5.8$ GPa, and $c_2 = 21.6$ GPa·s. But to model the total concrete strain, another spring $k_1 = 21$ GPa in series with the damper c_1 must be used to simulate the elastic modulus $E_{c_{28}}$, see Fig. 6. This four-element Burgers model is indeed capable of reproducing well the long-term mechanical behavior of the concrete whose creep data are given in Fig. 4. The secant

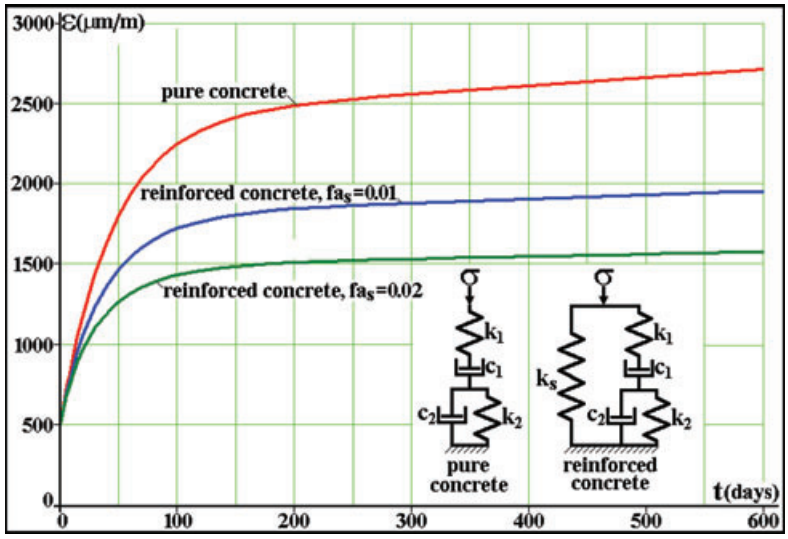

Fig. 6: Strain histories $\varepsilon(t)$ estimated by Eq. 11 for a pure concrete and for two steel reinforced concrete columns with steel area fractions fa_s = 1% and fa_s = 2%, when they are loaded by a fixed force that causes an initial strain ε_0=500 μm/m. The concrete is modeled as a linear viscoelastic Burgers material with constant parameters: k_1 = 21 GPa, c_1=1.814 TPa·s, k_2 = 5.8 GPa e, c_2=21.6 GPa·s, whereas the steel reinforcement is modeled as a Hookean material with k_s = 200 GPa

modulus $E_B(t)$ of the Burgers model is given by:

$$E_B(t) = \frac{k_1 c_1 k_2}{c_1 k_2 + c_1 k_1 [1 - exp(-k_2 t / c_2)] + k_1 k_2 t} \qquad (10)$$

However, to model a reinforced concrete column under pure compression, it is necessary to use still another spring in parallel with the Burgers model to describe the effect of the steel rods. Only one spring is needed because the steel creep can be neglected at room temperature. Also, this spring is in parallel with the concrete model because both see the same strains to maintain geometric compatibility. Therefore, if A_s is the total area of the reinforcing steel rods and A_c is the concrete area in a column whose cross-section area $A = A_s + A_c$, then $fa_s = A_s/A$ and $(1–fa_s)$ are the area fractions of the steel and the concrete in the column. If F is the force (supposed constant) which loads the column; E_s is the steel elastic modulus (which does not creep) and $E_c(t)$ is the (variable) creep modulus of the concrete; $\sigma_s(t)$ and $\sigma_c(t)$ are the stresses on the rods and on the concrete (both vary in time, since the concrete creep transfers loads to the steel reinforcing rods); and $\varepsilon(t)$ is the column strain (which also varies as time passes by), then it is trivial to show that the compressive force in the column is $F = \sigma_s(t)\cdot A_s + \sigma_c(t)\cdot A_c = \varepsilon(t)\cdot[E_s\cdot A_s + E_c(t)\cdot A_c]$, therefore:

$$\varepsilon(t) = \frac{F}{E_s A_s + E_c(t) A_c} = \frac{F/A}{fa_s k_s + \frac{(1-fa_s)}{1/k_1 + t/c_1 + [1-exp(-k_2 t/c_2)]/k_2}} \qquad (11)$$

It is also easy to show that the equivalent stress in the column is given by:

$$\sigma = F/A = \varepsilon(0)[fa_s k_s + (1 - fa_s)k_1] = \varepsilon_0[fa_s k_s + (1 - fa_s)k_1] \qquad (12)$$

The steel area in a reinforced concrete column is typically 1 to 2% of its total area. Knowing that the (elastic) ultimate strain in reinforced concrete structural design is usually assumed as $\varepsilon_{Uc} = 2000$ μm/m,[3] a column designed for an initial strain $\varepsilon_0 = 500$ μm/m can thus be considered representative of the problems found in practice. Using this value, Fig. 6 shows the strain time variations expected from a pure concrete column (with $f'_c = 18$ MPa and the viscoelastic properties obtained above), and from two reinforced concrete columns, one with a steel area fraction $fa_s = 0.01$ and the other with $fa_s = 0.02$. This figure demonstrates that strains in the order of $\varepsilon_{max} = 1500–2000$ μm/m are certainly not incompatible with typical working loads applied on reinforced columns made out of the concrete whose creep strains are described by Fig. 4. But this figure does not include several important details about the concrete properties, which had to be estimated in order to generate the information that supports this claim, a fact that decreases its power. However, a quite comprehensive report by Ziehl et al.[7] presents several such details, removing any doubts about the adequacy of this approach.

Ziehl and his colleagues studied if reinforced concrete columns with steel area fractions $fa_s < 1\%$, the minimum steel fraction required by the American standard,[8,9] could be used for structural purposes. They said that those existing

minimum fa_s requirements for columns were developed to prevent yielding of the reinforcement resulting from creep deformations in the concrete; that the tests used to support this limit were conducted decades ago, when steel yield strengths for reinforcing bars were approximately half of what is common today; and that a substantial reduction in the column steel area fraction might be possible with present-day materials, resulting in economic savings. Ziehl et al. cast several 203 mm (8′) diameter by 1219 mm (4′) long cylindrical columns made out of two concretes with nominal compressive strengths (at 28 days) of 28 and 56 MPa (4 and 8 ksi), with three steel fractions fa_s (0.36, 0.54, and 0.72%). They subjected them to a constant axial load $F = 0.4 f'_c A$ (the maximum load allowed by ACI and AASHTO standards[8,9]) in reduced-humidity enclosures, and measured their long-term axial deformations using electric resistive and mechanical strain gages. The load was applied through coil springs to provide the necessary compliance. Unloaded specimens were used to monitor temperature and shrinkage-related deformations. They presented plots of measured strain versus time, and compared the experimental results with an analytical model reported by ACI Committee 209.[10]

The columns were cast in cardboard molds, which were stripped 5 days after having poured the concrete. These columns were loaded between 14 and 28 days after casting. To determine the material properties, 4 × 8 and 6 × 12 inch test cylinders were also cast for every group of columns. These cylinders were tested for modulus of elasticity and compressive strength at 7, 14, 28, and 56 days after casting. The steel rods were tested for yield and ultimate strengths. Relative humidity and temperature were maintained between 30 and 60% and 10 and 43°C. The period required to load the columns for a length of time sufficient for the rate of creep to approach nearly zero was initially estimated to be close to 2 years, but in practice it was 15–18 months, depending on the specimens. Ziehl's report is particularly meticulous, and should be consulted for further details on concrete specifications and experimental procedures.[7] Figure 7 shows how the technique discussed above can quite reasonably fit some of their data. Other similar results can be found in Ref. 11.

DEALING WITH THE REINFORCED CONCRETE TIME-DEPENDENT $\sigma\varepsilon$ BEHAVIOR ON DEAD LOAD MEASUREMENTS

The simple viscoelastic model presented above did fit quite well data from Leet[3] and Ziehl et al.[7] Hence, it is reasonable to use it to speculate about the measured strains, and their use for calculating the dead service loads that were actually present on the instrumented columns. Linear stress analysis has long been safely used for design purposes, and nothing is apparently more reasonable than to also use it to describe the $\sigma\varepsilon$ concrete behavior. Thus, multiplying the measured strains by the concrete Young's modulus to obtain the stress and then the load that induced them is a natural temptation, particularly in uniaxially loaded columns. A Hookean model is certainly adequate for design purposes, and may be perfectly acceptable to correlate low or admissible stress/strain data measured in standard compression tests, which last a few minutes, but it cannot describe the long-term strain behavior under dead load, where the creep strains are not negligible. When cutting off the steel rods which have been embedded in the concrete for so long, all the strains they supported are released including, of course, the creep strains, which can be much higher than the initial elastic strain induced by the (safe) dead load, as demonstrated

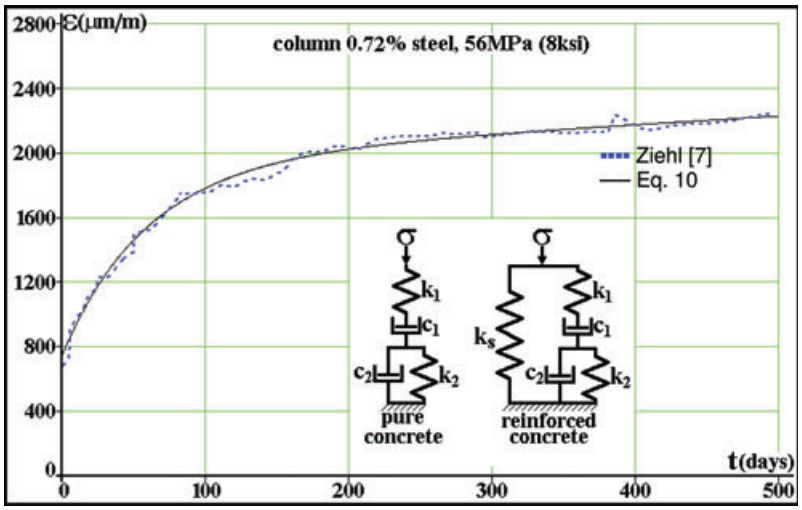

Fig. 7: Total (elastic plus creep) strain history $\varepsilon(t)$ estimated by Eq. 11 for a reinforced concrete column with f'_c=56 MPa and steel area fraction fa_s = 0.72%, loaded by a fixed force that induces an initial strain ε_0 = 800 μm/m : k_1 = 37.54 GPa, c_1 = 40 TPa·day, k_2 = 19 GPa, and c_2 = 1.2 TPa·day

above. Therefore, it must be strongly recommended that all released strain-based dead load measurements on concrete structures consider the creep influence.

However, in most practical cases, there simply is no information about the creep properties of the actual concrete cast in the instrumented structures. Therefore, designers should collect some concrete creep data if dead load measurements can be expected during the structure's service. As a simple four-element Burgers model may provide a reasonable description for the concrete creep data, as illustrated above, a practical way of accessing such data would be embedding strain transducers in some suitable structural members during their casting.

Or else, the only remaining option is to use some guidelines provided, for example, by ACI 209R "Prediction of creep, shrinkage, and temperature effects"[10] recommended practice to guess the creep properties, a much more imprecise procedure. Ziehl et al.[7] provides an interesting revision of such practices, which are quite involved, and there is no need to reproduce them here. Nevertheless, it is worth to mention that using the most reasonable assumptions for the cast concrete details in the ACI calculation routine, a mean initial strain of 585 μm/m was estimated for the instrumented reinforced columns, confirming that the measured values were indeed reasonable.

CONCLUSIONS

A relatively simple viscoelastic model was proposed to describe concrete creep, and extended to model the behavior of reinforced columns under axial loading. The model treats the concrete as a Burger's solid, composed by a Maxwell's element with a spring k_1 (which represents its elastic modulus) and a damper c_1, in series with a Kelvin–Voigt element whose spring is k_2 and the damper is c_2. The reinforcing steel is modeled by a spring k_s in parallel with the concrete. This model satisfactorily fitted column creep data from the literature, and can be used to explain why the measured residual strains were so high when compared with the nominal design strains. Based on these results, it is recommended that concrete creep properties should be measured when it is anticipated that dead load measurements can be necessary in the future.

References

1. Vieira, R.D., Castro, J.T.P., and Freire, J.L.F., "A New Technique for Measuring Loads in Concrete Columns," *Proceedings of the VI COTEQ*, Salvador, Brazil, in CD (2002) (in Portuguese).

2. Young, W.C., *Roark's Formulas for Stress and Strain*, 6th Edition, McGraw-Hill (1989).

3. Leet, K., *Reinforced Concrete Design*, 2nd Edition, McGraw-Hill, New York (1982).

4. Buyukozturk, O., "Creep and Shrinkage Deformation," MIT 1.054/1.541 Mechanics and Design of Concrete Structures Course Notes (2004).

5. Levenberg, K., "A Method for the Solution of Certain Non-linear Problems in Least Squares," *Quarterly of Applied Mathematics* **2**:164–168 (1944).

6. Marquardt, D., "An Algorithm for Least-squares Estimation of Nonlinear Parameters," *SIAM Journal on Applied Mathematics* **11**:431–441 (1963).

7. Ziehl, P.H., Cloyd, J.E., and Kreger, M.E., "Evaluation of Minimum Longitudinal Reinforcement Requirements for Reinforced Concrete Columns," Federal Highway Authority, Houston, TX, Report FHWA/TX-02/1473-S (1998).

8. ACI Committee 318, *Building Code Requirements for Reinforced Concrete and Commentary,* ACI, Detroit, MI (1995).

9. American Association of State Highway and Transportation Officials, *Standard Specification for Highway Bridges,* 15th Edition, AASHTO, Washington, DC (1992).

10. ACI 209-R86, *Prediction of Creep, Shrinkage, and Temperature Effects in Concrete Structures,* ACI, Farmington Hills, MI (1986).

11. Castro, J.T.P., Vieira, R.D., Sousa, R.A., Meggiolaro, M.A., and Freire, J.L.F. "Time-Dependent Residual Stresses in Reinforced Concrete Columns," *Proceedings of the SEM XI International Congress on Experimental and Applied Mechanics*, Orlando, FL, June 2–5, in CD (2008). ■